ISSN 2176-5480

22nd International Congress of Mechanical Engineering (COBEM 2013)
November 3-7, 2013, Ribeirão Preto, SP, Brazil

NUMERICAL AND EXPERIMENTAL ANALYSIS OF RIVETED JOINTS FOR AERONAUTICAL APPLICATIONS

André Ferrara Carunchio
Instituto de Pesquisas Tecnológicas do Estado de São Paulo – Av. Professor Almeida Prado, 532 São Paulo SP
fcarunchio@ipt.br

Larissa Driemeier
Escola Politécnica da Universidade de São Paulo - Av. Prof. Mello Moraes, 2231 São Paulo SP
driemeie@usp.br

Roberto Ramos Jr.
Escola Politécnica da Universidade de São Paulo - Av. Prof. Mello Moraes, 2231 São Paulo SP
rramosjr@usp.br

Rynaldo Zanotele Hemerly de Almeida
Instituto de Pesquisas Tecnológicas do Estado de São Paulo – Av. Professor Almeida Prado, 532 São Paulo SP
rynaldo@ipt.br

Willy Roger de Paula Mendonça
Embraer – Av. Brigadeiro Faria Lima, 1399 São José dos Campos SP
willy.mendonca@embraer.com.br

Abstract. *Riveted joints are widely used in many applications in industry to create permanent unions between structural members. In some aspects, this kind of union has a superior performance when compared to other connections, like glued bond joints (which have lower mechanical and thermal resistances) and screwed joints (which may have an inferior performance to fatigue behavior). Nonetheless, due to their geometrical characteristics, stress concentrations inevitably occur, which contributes to fatigue crack initiation and, eventually, to a catastrophic failure. Today, the vast dissemination of finite element codes makes the numerical analysis of these joints much more expeditious. On the other hand, if not well conducted, FE analyses become expensive and laborious, besides generating results not always satisfactory. In this work, 3D numerical models of riveted joints produced according to aeronautic procedures and requirements were built, employing different parameter and strategies. The results were compared to experimental data, obtained from test machine transducers (force and displacement) and the use of strain-gages, with the purpose of comparing the models' performance from the accuracy and computational cost point of views. Thus, the aim of this work is to determine the best procedure to conduct a FE analysis of a riveted joint, and which parameters must be considered to reach accurate and reliable results.*

Keywords: *riveted joints, finite element, aeronautical structures.*

1. INTRODUCTION

Riveted joints are widely used in many applications in industry to create permanent unions between structural members. In some aspects, this kind of union has a superior performance when compared to other connections, like glued bond joints (which have lower mechanical and thermal resistances) and screwed joints (which usually have an inferior performance to fatigue behavior). Nonetheless, due to their geometrical characteristics, stress concentrations inevitably occur, which contributes to fatigue crack initiation and, eventually, to a catastrophic failure (MÜLLER, 1995).

In order to improve the design of riveted joints, many experiments must be carried out but they are expensive, time consuming, and do not allow the instrumentation of critical areas of the riveted joints. Since there are eccentricities in this kind of joints, secondary moment occurs (SHIJVE, 2009; MÜLLER, 1995), which increases the tension stress in the interface between sheets in a lap joint configuration, or between sheets and splice in a butt joint configuration. These areas cannot be monitored with standard strain transducers such as strain gages or photoelastic resin. Thus, finite element modeling may be an important tool for extrapolation of stress and strain fields to these critical non instrumented areas of the joint in order to create useful data for the design of riveted joints from the fatigue point of view (SHIJVE, 2009; KUMAR, *et al*., 2012).

Most of finite element models found in the literature are based on 2D elements to represent joint sheets, and springs or beams to represent rivets (KUMAR, *et al*., 2012; BEDAIR and EASTAUGH, 2007). The major difference among the 2D models is related to the elements or the parameters used for modeling the load transfer between sheets and idealized rivets. This is a key subject for achieving good simulation results (BEDAIR and EASTAUGH, 2007). Although simple,

ISSN 2176-5480

these models are enough accurate and computationally efficient to be employed on the design of large panels with riveted joints considering the ultimate strength criteria (KUMAR, *et al*., 2012).

Some works were based on 3D elements, aiming to develop more accurate models. In (EKH, 2006) an elaborated model of a bolt shear joint was developed accounting for clearance, bolt clamp-up and friction effects. (PARK, 2007) used 3D modeling for crack growth analysis at sheet holes in riveted joints. These models are interesting for their original investigation but their employment on large panel analysis is not feasible (KUMAR, *et al*., 2012; EKH, 2006).

Today, the vast dissemination of finite element codes makes the numerical analysis of these joints much more expeditious. On the other hand, if not well conducted, FE analyses become expensive and laborious, besides generating results not always satisfactory. This work presents some investigation on the modeling of riveted joints using 3D finite elements and contact tools, as analytic contact, to improve the results accuracy. The main objective is to determine good procedures to conduct a 3D FE analysis of a riveted joint, and to identify which parameters and effects must be considered to reach accurate and reliable results.

At least three applications would be benefited with 3D refined models. The first one is the fatigue analysis that could be based in more realistic stress field data. The second is the design of critical structure sections, in which computationally cost models may be considered feasible. And in a third application, the complete 3D model may be used as a benchmark for simpler 2D models assessment.

In the following sections the joint under investigation is shown, finite element modeling and experimental procedures are presented in detail, simulation results and experimental data are compared, and future steps on the refinement of the modeling are discussed.

2. MATERIALS AND METHODS

2.1 Joints Description

The specimens used in this work were produced with the intention of representing the riveted joints commonly applied in aircrafts. Therefore, their dimensions, materials, manufacturing processes and other characteristics were chosen based on the current aeronautic industry practices.

Asymmetrical butt joints made in 2524-T3 aluminum alloy were used in this research, with 1.6 mm thickness sheets and 2 mm thickness splices. 4 mm (5/32”) Brilles fasteners, made in aluminum 2117-T4, according to NASM 14218 standard, are responsible for joining the sheets, as shown in Fig. 1 (a).

For some preliminary studies of the joint behavior, specimens with the same characteristics but with only six rivets rivet, as shown in Fig. 1 (b). This procedure also allowed the use of simpler and faster solution finite element models, a desirable condition for initial simulations and model formulation.

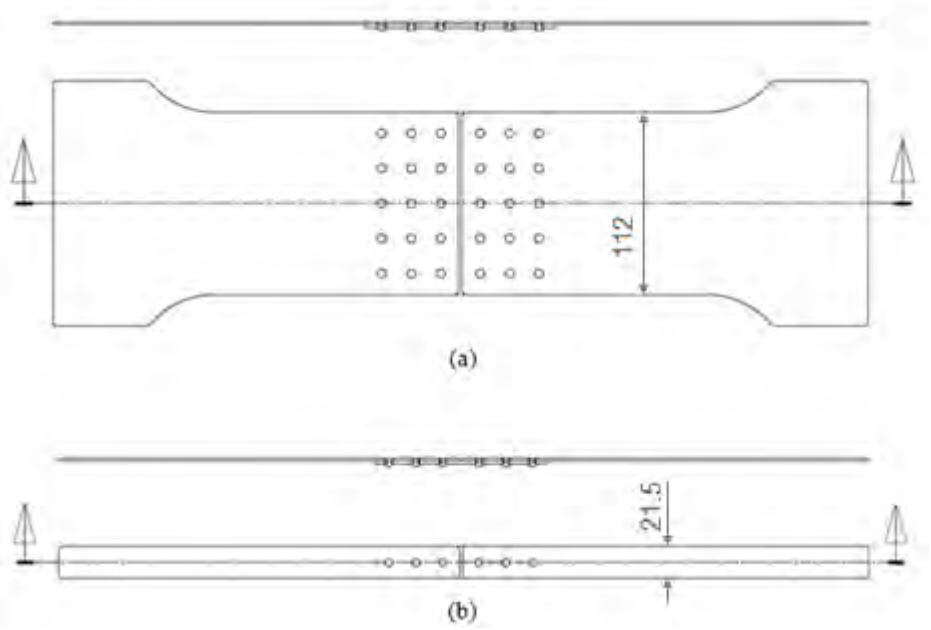

Figure 1. Specimens configurations: (a) wide joint; and (b) narrow joint

2.2 FEA Procedures

The software used for the finite element analysis was the MSC Patran 2010, configured to use MSC Marc as solver. Patran offers two different options to define the boundary of contact bodies: discrete or analytic, which were both

ISSN 2176-5480

studied since establishing the influence of this choice in the analysis results was one of the objectives of this part of the work. According to MSC's manuals (MSC.SOFTWARE, 2010), the contact interaction is defined, among other factors, by a constant normal vector of a segment. However, the real structure may be curved with a variable normal vector, what leads to inaccuracies in the results. As an alternative, it is possible to describe the outer surface of a body with an analytical expression, what improves the geometric representation and the calculation of the normal vector, providing more realistic results.

To exemplify the explanation of these two technics described previously, a simulation was carried out to show the differences in a contact analysis. The model (shown in Fig. 2 a) consists in a cube with a through hole, in which a pin is assembled. Both extremities of the pin had all of their degrees of freedom constrained, while a tensile force was applied in one of the surfaces of the cube in the X direction. Figures 2 (b) and (c) show the stress in X direction in the pin with analytic and discrete contact definition, respectively. It is possible to observe that the analytic boundary gives a better distributed stress field, with the highest values of compressive stresses (dark blue) in the region in contact to the edge of the cube's hole, and it decreases approaching the middle of the model. On the other hand, the discrete boundary (Fig. 2 c) gives an unexpected stress field; moreover, it was verified that the stress values were higher in the last simulation, probably due to a worse force distribution in the nodes.

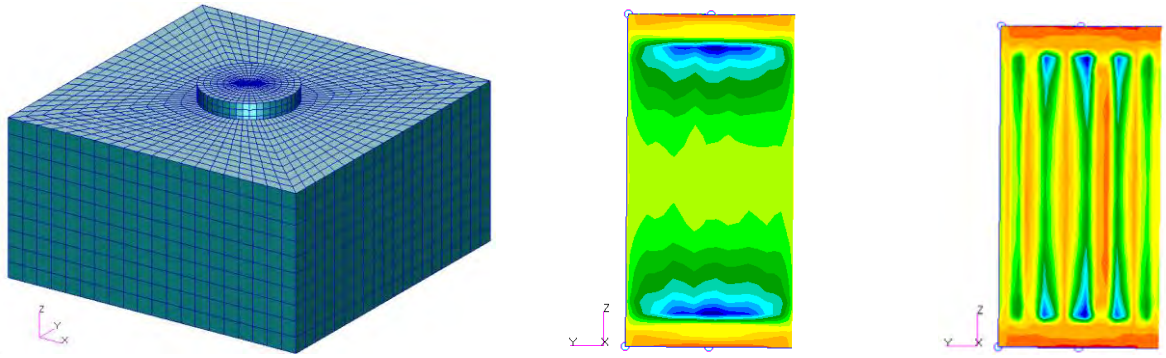

a) b) c)

Figure 2. (a) model to test boundary types; (b) Stress in the X direction with analytic boundary; (c) Stress in the X direction with discrete boundary

The joint model's geometry was built similar to the specimens. The material was considered isotropic with bilinear relation between stress and strain. The model also did not include any friction effects, neither rivet's interference or clamping force, although it is known they have a considerable role in joint fatigue performance (MÜLLER, 1995). As the specimens present two symmetry planes, and they are also subject to symmetrical load, the model can take advantage of this fact and be reduced to only one quarter of the joint, as shown in Fig. 3 a.

The sheet's mesh was built using 8 nodes hexahedral elements, and in the high stress gradient areas the element edge length was set to 0.19 mm. For the fasteners, 4 nodes tetrahedral elements were used with approximately the same discretization, what resulted in 24092 elements in the entire model, as can be seen in Fig. 3 b.

To make possible the comparison between the symmetrical model and the experimental results of an entire joint, the displacements in Z direction (according to Fig. 3 orientation) were constrained for all nodes contained in the XY symmetry plane, as well as the displacement in X direction for all nodes in the YZ symmetry plane. In the other extreme of the joint, the only degree of freedom that was set free was the X direction, to model the machine's grip. In this location, a distributed load of 3584 N was applied.

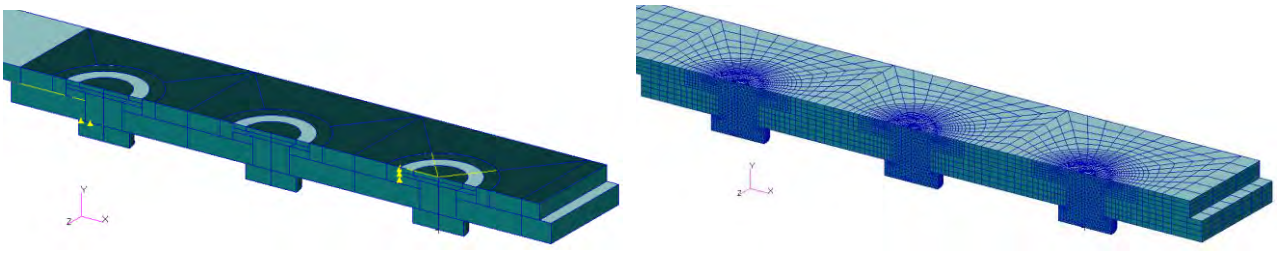

a) b)

Figure 3. Use of symmetry in the finite elements models

Besides the type of contact, another factor that was investigated was the influence of the application point (mesh or geometry) of this boundary condition. Therefore, different analyses were performed and their characteristics are defined in Tab. 1. One of the jobs (named A4) was carried out using the "initial contact" tool, which is recommended by MSC's manuals (MSC.SOFTWARE, 2010) in some situations where contact exists in the beginning of the analysis.

ISSN 2176-5480

Table 1. Jobs' description of narrow model

Name	Contact		Solving time (s)
	Contact type	Application region	
A1	Discrete	Mesh	7319
A2	Analytic	Mesh	4155
A3	Discrete	Geometry	3492
A4	Discrete	Geometry	3908
A5	Analytic	Geometry	Failed to converge

The model for the wide specimen, in Fig. 4 was geometrically a continuation of the narrow model. The construction was easily conducted with the use of drawing tools as "mirror" and "translate". The only difference in this model was the applied load, that changed to 27,5 kN. All the boundary conditions were kept the same.

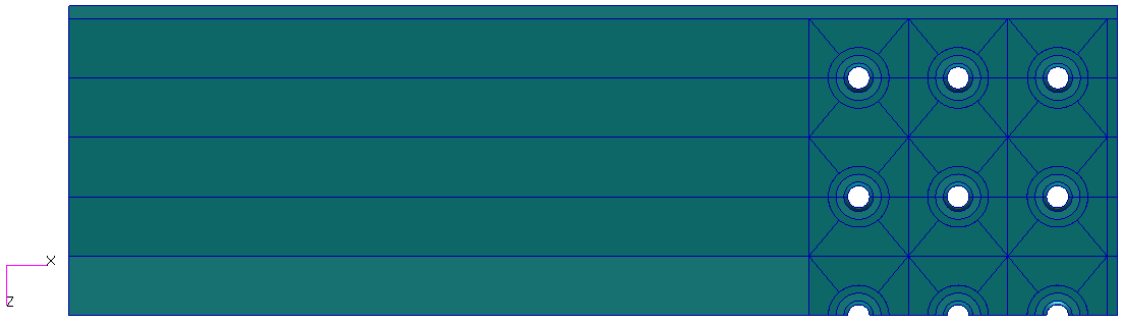

Figure 4. Wide model's geometry

2.3 Experimental Procedures

Two narrow specimens were tested under constant crosshead speed of 0.1 mm/s, up to the joint rupture. The wide specimen load profile, on the other hand, was composed by four constant load levels intercalated with load ramps, as illustrated in Fig. 5, up to the joint rupture. Those levels were defined in order to impose 40 MPa, 80 MPa, 160 MPa, 200 MPa, nominal tension stress (in the gross cross-section area) on the specimen and the load ramps' rate was equivalent to 4 MPa/s.

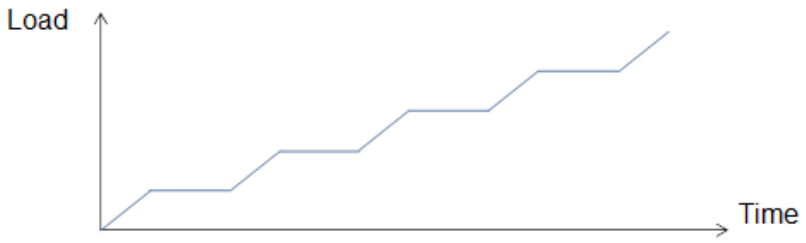

Figure 5. Time versus load diagram

The wide specimen was instrumented with 3 millimeters grid strain gages, specifically positioned as depicted in Fig. 6 to capture different phenomena: S3 and S14 are located each one in a face of the splice, to monitor the effect of the secondary bending; the other gages are situated between the holes, to monitor the strains in a low gradient area, and thus, avoiding the uncertainties of measuring strains near the holes (high gradient area).

ISSN 2176-5480

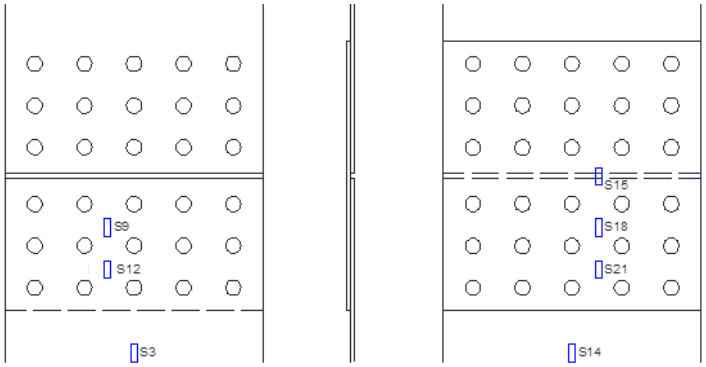

Figure 6. Strain gages position in the wide joint

3. RESULTS

3.1 Narrow model

Evaluating the results of the simulations, it was noted that the stress fields and magnitudes were approximately the same for all models (A1 to A4). The narrow joint was not instrumented with strain gages, so the only data available to compare with the numerical model that obtained from test machine load and displacement transducers, according to Fig. 7.

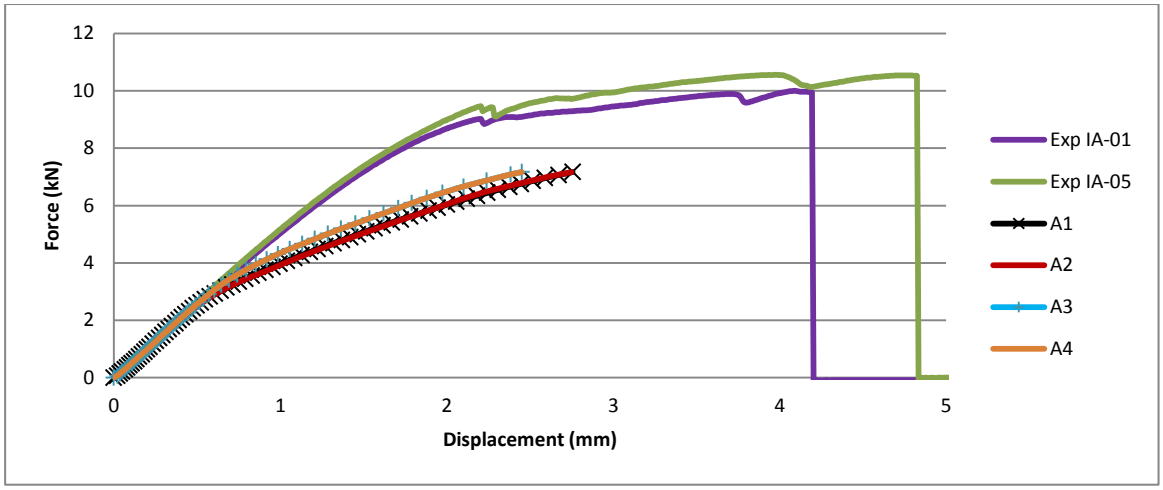

Figure 7. Diagram of force versus displacement for comparison between numerical and experimental results

Analyzing Fig. 7, it is possible to see that all models are representative under small loads, up to 2 kN approximately, interval in which all of them have similar behaviors. Furthermore, it is notable that the contact surface type (discrete or analytic) does not influence the joint's behavior. The differences in the force x displacement curves due to the form in which contact was applied (mesh or geometry) are small but unexpected. Models A3 and A4 - with contact defined in the geometry - are closer to the real joint performance. No differences in the results were noticed for the model A4, which used the initial contact tool.

Figures 8 and 9 show the stresses in X direction.

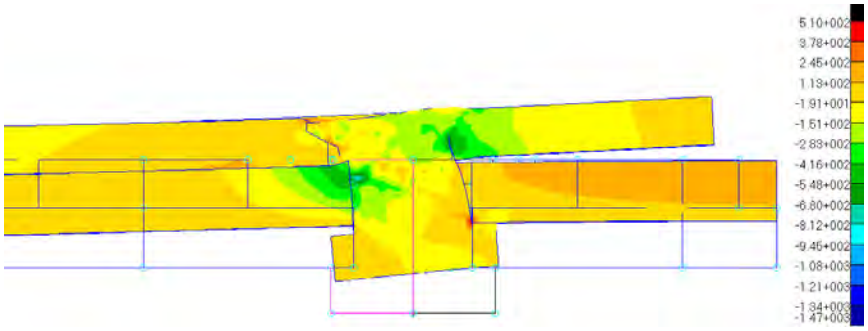

Figure 8 – Stresses in X direction in the joint - side view (detail)

ISSN 2176-5480

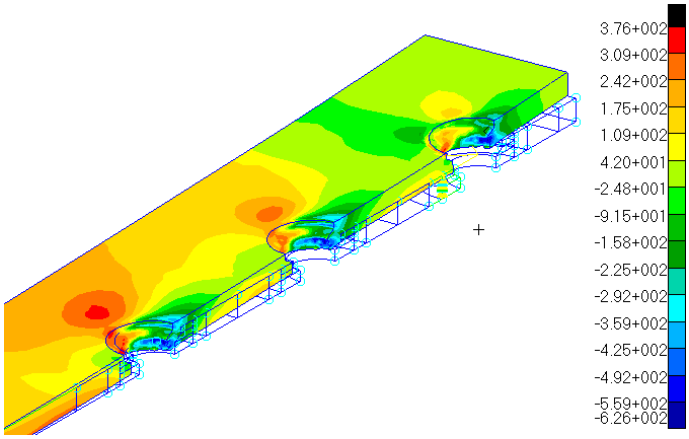

Figure 9 – Stresses in X direction in the splice - isometric view (detail)

It is possible to see in Fig. 8 that the highest values of stress in the symmetry plane are located closer to the interface of the joint. This happens because this section receives a more intense contact from the rivets, since they are under a considerable deformation. The rivet flexibility also influences the distribution of the load of different rows, as explained by MÜLLER (1995).

During the experimental procedure, both specimens collapsed due to rivets shear, as shown in Fig. 10. It was also noticed in the experiments the tendency of the rivets' heads to penetrate the sheets, as seen in the finite element models.

Figure 10. Narrow specimen after the test

3.2 Wide Joint

The simulation of the model for the wide joint was carried out using discrete contact applied in the geometry, considering that this option was the fastest for the narrow joint, and all of them had similar results. The job failed to converge and was automatically aborted at 43 percent of the progress (equivalent to a 23,65 kN load for the entire joint), however it was possible to obtain some data. Figures 11 and 12 show the stresses in X direction.

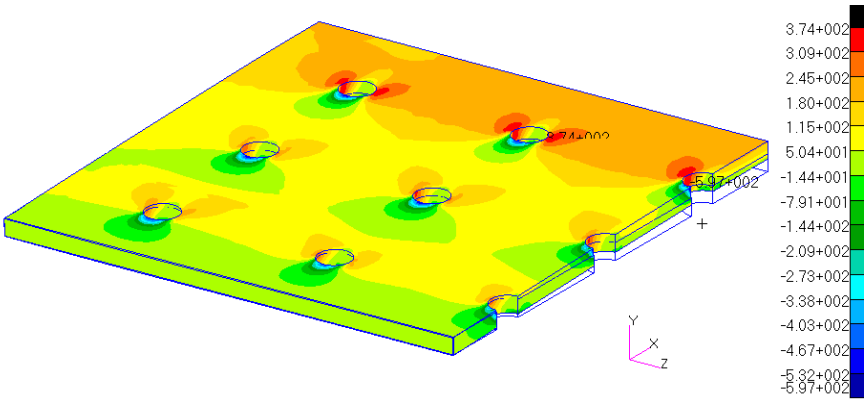

Figure 11. Stresses in X direction in the splice - isometric view

ISSN 2176-5480

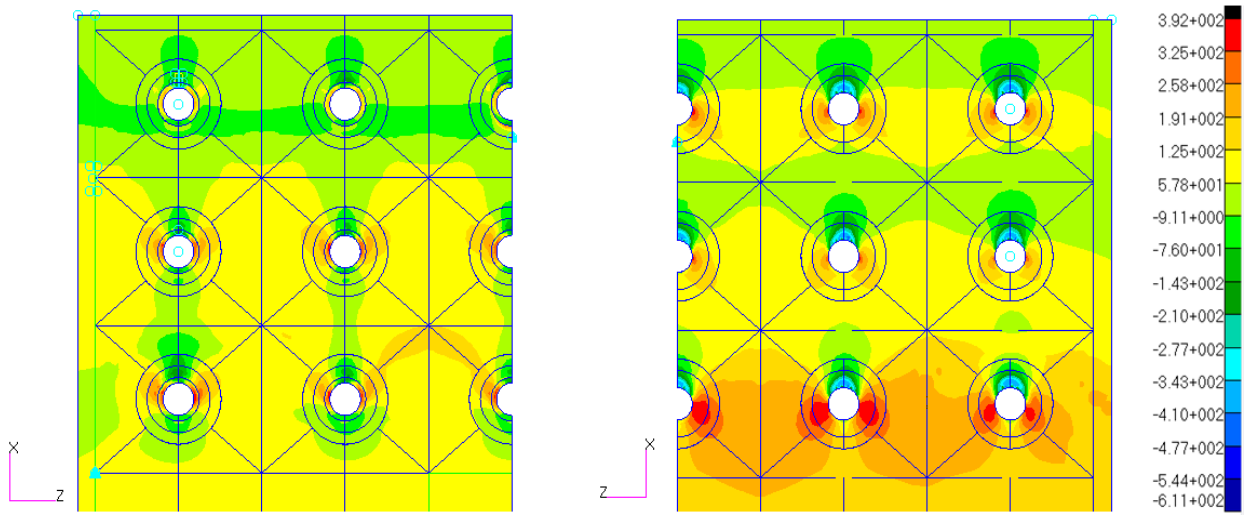

Figure 12. – Stresses in X direction in the splice – top view (left) and interface (right)

It is possible to observe that the most loaded row in the sheet was the furthest from the joint's center, while in the splice was the nearest one. As expected, the instrumented face had lower stresses than the interface, as in the narrow model, what appears in Fig. 11 and 12. Figure 13 was built showing the stress in X direction in each node located in the top face and in the interface of the XY symmetry plane.

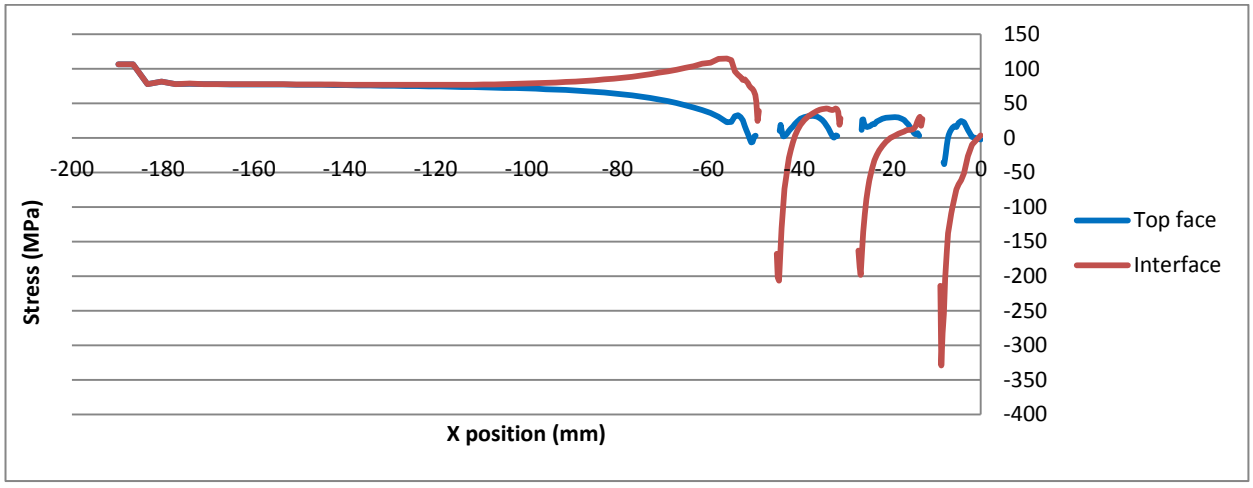

Figure 13. Stress in X direction in the XY symmetry plane

Approaching the riveted area, it is possible to see the effect of the secondary bending, compressing the top face and tensing the interface, until get close to the first roll of fasteners, where the σ_x stress at the top face decreases to almost zero. Then, the interface gets strongly compressed by the action of the rivet's contact force, while on the top the stress value is lower. The same behavior is observed after the other two rows of rivets.

As well as the narrow models, it was made a comparison between load and displacement in the experiment and in the simulation. As is shown in Fig. 14 a, the model is representative only under small loads, until approximately 12.5 MPa. It was also made a comparison between the model's deformations and those obtained from the strain gages (see Fig. 14 b to h).

ISSN 2176-5480

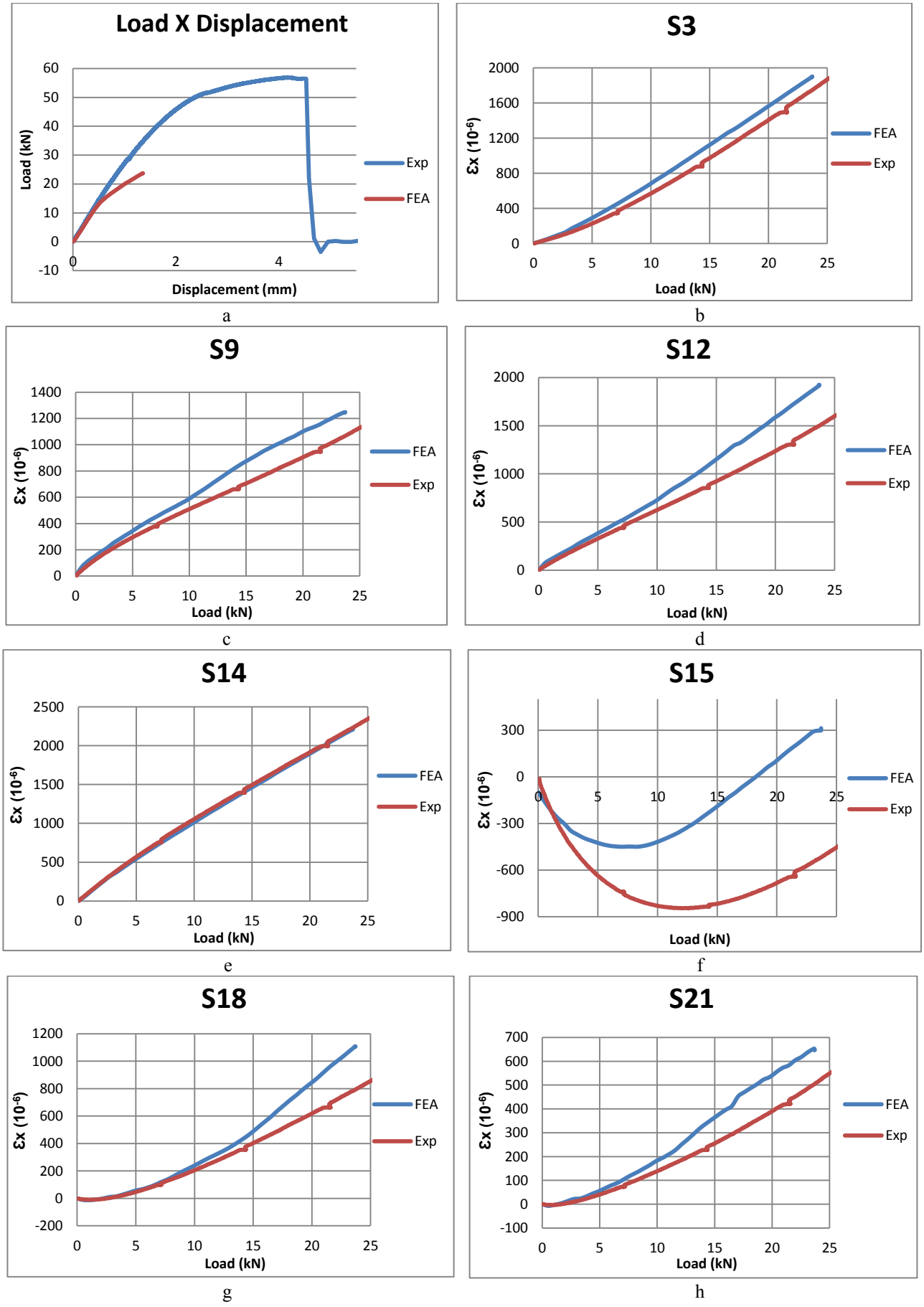

Figure 14. Test machine's transducer, strain gage data and numerical results for the wide joint

ISSN 2176-5480

By the graphics exposed it is possible to observe that, in general, the numerical model had similar results compared to the experimental tests, especially for lower loads.

4. CONCLUSIONS

3D finite element models were developed using different strategies and tools, in order to understand their influence in the results. Regarding the type of contact – discrete or analytic - it was noticed that despite a considerable local difference in the stress field, the global behavior of the joints did not change significantly. Therefore, analytic contact is recommended when specific areas of a structure (contact areas) are studied, or whenever a more accurate analysis is required. Moreover, the application of the contact in the geometry seemed to be a better option since it provided faster and more accurate solutions for this problem.

Experimental tests were carried out using riveted joints produced according to current aeronautic industry procedures, obtaining data from the specimens by the test machine transducers and strain gages. The comparison between this data and the numerical calculation showed that the finite element model was accurate for small loads, but as it increases, divergences occur. These variations may happen due to other phenomena that were not included in the models, such as friction and squeeze force. Numerical instabilities during the model solution are another possibility to explain the divergences that cannot be discarded. Furthermore, with the use of more specimens for the experimental procedures the comparisons could be improved.

The finite element model showed that the highest stresses are located in the interface between the sheets and the splice, which is also the region where crack initiation occurs in the case of dynamic loads. Thus, despite instrumentation data is an important tool during research or design stage, it is advisable to extrapolate stress and strain fields to these critical regions.

5. REFERENCES

Bedair, O.K. and Eastaugh, G.F., 2007. “A numerical model for analysis of riveted splice joints accounting for secondary bending and plates/rivet interaction”. *Thin-Walled Structures*, Vol. 45, p.251

Ekh, J. and Schön, J., 2006. “Load transfer in multirow, single shear, composite-to-aluminium lap joints”. *Composites Science and Technology*, Vol. 66, p.875-885

Marc user’s manual Vol. A, version 2010, MSC.Software Corporation

Müller, R.P.G., 1995. *An experimental and analytical investigation on the fatigue behavior of fuselage riveted lap joints*. Dr. thesis, Delft University of Technology, Delft.

Kumar, D.V.T.G.P., Naarayan, S.S., Sundaram, S.K. and Chandra, S., 2012. “Further numerical and experimental failure studies on single and multi-row riveted lap joints”. *Engineering Failure Analysis*, Vol. 20, p.9-24

Park, C.Y. and Grandt, A.F., 2007. “Effect of load transfer on the cracking behavior at a countersunk fastener hole”. *International Journal of Fatigue*, Vol. 29, p.146-157

Schijve, J., Campolini, G., Monaco, A., 2009. “Fatigue of structures and secondary bending in structural elements”. *International Journal of Fatigue*, Vol. 31, p.1111-1123

6. RESPONSIBILITY NOTICE

The authors are the only responsible for the printed material included in this paper.